Iranian Journal of Chemical Engineering
Vol. 9, No. 2 (Spring), 2012, IAChE

Research note

Solution of Noncatalytic Packed Bed Reactors Equations by Finite Element Method

A. Afshar Ebrahimi, H. Ale Ebrahim[*]
Department of chemical engineering, Amirkabir University of Technology (Tehran Polytechnic), Petrochemical Center of Excellency, Tehran, Iran

Abstract

The partial differential equations describing reaction of a trace component in the gas stream in a packed bed of solid reactant or adsorbent are solved by Rayleigh-Ritz finite element method. These equations consist of a PDE along the reactor which is accompanied with semi time dependent diffusion-reaction equation in each pellet. Two gas-solid reaction models have been considered as the reaction rate expression of the pellets in this work. These reaction rates provide nonlinearity in the PDEs of the pellets. Reactions with considerable structural changes such as sulfation of calcined limestone in packed column have been considered too. The finite element method analyzed the PDEs equations, even in the presence of steep gradients associated with nonlinearities along the packed column and the pellets equations.

Keywords: *Finite Element Method; Rayleigh-Ritz; Nonlinear Partial Differential Equations; Non-catalytic Packed Bed Reactors*

1. Introduction

Gas-solid reactions are important in many chemical and metallurgical industries. The most important applications of gas-solid reactions are as follows:

1. Reduction of metallic oxides [1-3].
2. Roasting of metallic sulfides [4, 5].
3. Adsorption of acid gases by solids [6-9].
4. New method for synthesis gas production [10].
5. Barium carbonate preparation [11].
6. Active carbon production [12,13].
7. Coal gasification process [14,15].

Adsorption or reaction in packed beds of solid reactants or sorbents is widely used for purification or separation of gases in many industries, especially for removing the trace of H_2S from natural gas in the entrance of petrochemical plants. As a result of contact between gas and solid in a packed bed, a reaction front forms which gradually moves along the column. To design a packed bed, one needs to know the time for which the solid can be exposed to the gas before breakthrough of undesired gas components leave the column. In other words, the time which the reaction front reaches the top end of the packed column has a significant role in

* Corresponding author: alebrm@aut.ac.ir

the performance of a packed bed reactor. Thus, a comprehensive modeling and accurate solution of the equations of the model leads to acceptable results for designing a packed bed reactor. There are extensive efforts on the modeling of adsorption process in packed beds [16,17]. In addition to this, there are numerous works on developing and solving the equations of the reaction of a single pellet with gas [18-24]. Liapis and Rippin [25] used orthogonal collocation for solving equations describing the simultaneous adsorption of two components in a packed column. Fernandes and Gavalas [26] extend a semi analytical technique of Del Borghi et al. [19] and Dudukovic and Lamba [20] to reactions in packed beds.

In this work, the equations of the gas-solid reactions (or adsorptions) in packed beds are solved by Rayleigh-Ritz finite element method successfully. Some computer codes have been developed for this purpose in MATLAB. These computer codes are able to solve these equations successfully with various mesh numbers, even in the presence of high gas concentration gradients accompanied with nonlinearities. Two famous models in gas-solid reactions known as volume reaction model and random pore model have been considered in this work. Among these models, random pore model is applicable for the reactions (or adsorptions) with structural changes. In this work the reaction of sulfur dioxide with calcined limestone (with structural changes) in a packed bed has been surveyed. Therefore, the behavior of the reaction front in the packed columns (accompanied with incomplete solid conversion) is investigated successfully. In addition, the adsorption reaction of $ZnO+H_2S$ in a packed column is being considered. In the case of volume reaction model in the bed, results of this work reveal acceptable agreement with the results of Fernandes and Gavalas [26].

The Rayleigh-Ritz finite element method is a robust method in the engineering problems and can accurately handle sophisticated reaction equations of a packed bed in the presence of steep gradients in the solid pellets or along the bed. This method avoids the discretization of the differential operators, thus reducing numerical instabilities. Moreover, the gas and solid concentration profiles are available along the bed and within the solid reactants by this method in all positions in the bed.

2. Mathematical modeling

The general form of a gas-solid reaction is as follows:

$$A(g)+\upsilon_B\, B(s)\rightarrow C(g)+\upsilon_D\, D(s) \qquad (1)$$

The governing dimensionless equations describing a packed column are as follows [26]:

$$\frac{\partial^2 y}{\partial \xi^2}-Pe\,\frac{\partial y}{\partial \xi}=\beta\left(y-\zeta\,|_{\rho=1}\right) \qquad (2)$$

where y is the dimensionless bulk gaseous concentration through the reactor, ξ is the dimensionless reactor coordinate, Pe is the Peclet number, β is a dimensionless parameter which is defined in the

nomenclature and $\zeta|_{\rho=1}$ is the gas concentration at the surface of the solid reactants along the bed.

$$\xi = 0: \ \frac{\partial y}{\partial \xi} = Pe\,(y - 1) \tag{3}$$

$$\xi = \Lambda: \ \frac{\partial y}{\partial \xi} = 0 \tag{4}$$

$$\frac{1}{\rho^2}\frac{\partial}{\partial \rho}\left(\rho^2 \frac{\partial \zeta}{\partial \rho}\right) = \phi^2 f\,(b)\,\zeta \tag{5}$$

where ρ is the dimensionless radius of the spherical pellets in the reactor, ζ is the dimensionless gaseous concentration in each pellet, ϕ is the reaction Thiele modulus and $f(b)$ is the reaction function depending on dimensionless solid concentration.

$$\rho = 0: \ \frac{\partial \zeta}{\partial \rho} = 0 \tag{6}$$

$$\rho = 1: \ \frac{\partial \zeta}{\partial \rho} = Bi\,(y - \zeta) \tag{7}$$

$$\frac{\partial (b \text{ or } r^*)}{\partial \tau} = -f\,(b)\,\zeta \tag{8}$$

where τ is the dimensionless time.

$$\tau = 0: \ b = 1 \tag{9}$$

All of the dimensionless parameters are also defined in the notation.

Eq. (2) is the mass conservation of the gaseous reactant along the bed. Eq. (5) is the gas conservation in the solid pellet where the reaction takes place. Finally, Eq.(8) shows the variation of the local solid concentration in the pellet with progress of time. $\zeta|_{\rho=1}$ is the coupling term of Eqs. (2) and (5). This term is the gas concentration at the surface of the solid reactants along the bed.

The following assumptions have been considered in the above modeling:

- The gas phase accumulation terms in the bed and pellet have been neglected [26,27].
- The size of the pellets remains unchanged during the reaction.
- The reaction is first order with respect to the gaseous reactant.
- The reaction is irreversible and the system is isothermal.

3. Finite element method

Since the reaction in each pellet is symmetric with respect to the center of the spherical solid reactants, the spherical solid pellets in the bed are divided to the uniform mesh from the center of the pellet up to the surface. Also, the length of the packed column is divided to the uniform mesh from the bottom of the bed up to the top end.

The solution procedure of Eqs. (2) to (9) is depicted in Fig. (1). Solution procedure of Eqs. (2) and (5) are as follows:

Consider a typical element in the bed $\Omega_e(\xi_a, \xi_b)$, whose endpoints have the coordinates $\xi = \xi_a$ and $\xi = \xi_b$, is isolated from the mesh. The weighted integral form of Eq. (2) over this element is as follows:

$$\int_{\xi_a}^{\xi_b} w\left[\frac{\partial^2 y}{\partial \xi^2} - Pe\frac{\partial y}{\partial \xi} - \beta y + \beta \zeta|_{\rho=1}\right] d\xi = 0 \tag{10}$$

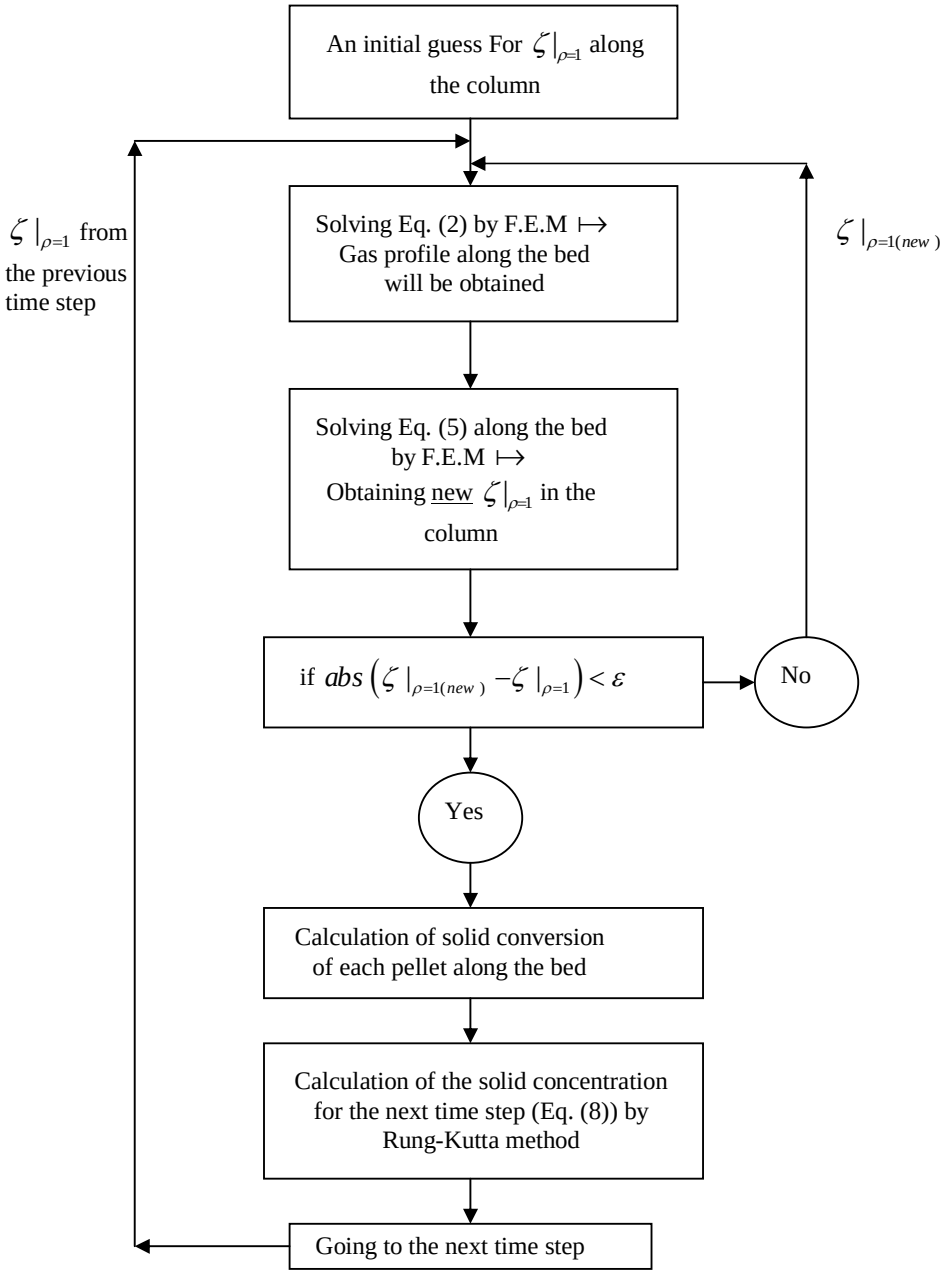

Figure 1. diagram box of the solution procedure of Eqs. (2) - (9)

Where w denotes the weight function. Integration by parts is used on first term in the bracket of Eq. (10) to distribute the spatial derivative equally between the weight function w and the dependent variable y .

$$-w\,\frac{\partial y}{\partial \xi}\Big]_{\xi_a}^{\xi_b} + \int_{\xi_a}^{\xi_b}\left(\frac{d\,w}{d\,\xi}\frac{d\,y}{d\,\xi} + Pe\,\frac{\partial\, y}{\partial \xi} + \beta\, y - \beta\,\zeta|_{\rho=1}\right) d\,\xi = 0 \qquad (11)$$

Eq. (11) is the weak form of the differential equation. The first term in the above equation is related to natural boundary conditions in the nodes of the typical element. The bulk gas concentration (dependent variable) in each mesh is defined as follows:

$$y = \sum_{j=1}^{3} y_j^e \, L_j^e \tag{12}$$

Where L_j^e are the one dimensional Lagrangian interpolation functions over the element of the column [28]. y_j^e are the unknown nodal values of the bulk concentration in the typical element of the bed. Inasmuch as quadratic interpolation functions have been employed for each element in this work, each mesh has three unknown nodal points.

In the Rayleigh- Ritz method we have [28,29]:

$$w = L \tag{13}$$

Substituting Eqs. (12) and (13) into Eq. (11) leads to the following algebraic system of equations in a typical element of the bed:

$$\left[K^e\right]\left\{y^e\right\} = \left\{Q^e\right\} \tag{14}$$

Where

$$K^e = \int_{\xi_a}^{\xi_b} \left(\frac{d\,L_i}{d\,\xi}\frac{d\,L_j}{d\,\xi} + Pe\,\frac{d\,L_j}{d\,\xi} + \beta\,L_j - \beta\,\zeta\,|_{\rho=1} \right) d\,\xi$$

$$i = 1,2,3 \quad j = 1,2,3 \tag{15}$$

The above equation is the coefficient matrix for a typical element in the column. It should be noted that the term $\zeta\,|_{\rho=1}$ in Eq. (15) is defined by guess (see Fig. 1). For instance, when there are 100 elements along the bed, there are 201 nodes in which the surface gas concentration at these nodes must be defined as an initial value. These values were assumed 1 in all nodes along the bed in the beginning of all runs. After 3 or 5 iterations, the surface concentration along the bed converged to its correct values.

$\left\{y^e\right\}$ is the unknown nodal vector of bulk concentration in the element and $\left\{Q^e\right\}$ is the right hand side vector which is defined by the boundary conditions of the element. Assembling Eq. (15) leads to an algebraic system of equations for the entire unknown global nodal vector of bulk concentration in the bed:

$$\left[K\right]\left\{y\right\} = \left\{Q\right\} \tag{16}$$

Where $\left[K\right]$ is the assembled global coefficient matrix and $\left\{Q\right\}$ is the global right hand side vector. This vector shows the flux of mass transfer in the bed. All components of $\left\{Q\right\}$ are zero except the first component due to the boundary condition in the entrance of the bed.

As the solid concentration is known in each pellet at the initial time, the gas concentration profile will be obtained by finite element method in the solid pellets in the bed. The solution procedure is similar to the solution of the bulk gas concentration in the bed i.e.

constructing the weighted integral form of Eq. (5), integrating by parts and obtaining the weak form of the Eq. (5), substituting Eqs. (12) and (13) into the weak form, assembling the element equation, imposing boundary conditions and finally solving the algebraic system of equations for the gas concentration in the pellets. The solid concentration for the next time step within the pellets in the column will be calculated by employing fourth order Rung-Kutta method on the Eq. (8).

4. Results and discussion

In this section, results of this work are presented for two gas-solid reaction models.

4.1. Volume reaction model

In this model the reaction is first order with respect to the reacting sites in the solid. The function f takes the simple form as follows:

$$f(b) = b \tag{17}$$

Figs. (2) through (4) are the comparison of this work with the semianalytical technique of Fernandes and Gavalas [26]. In Fig. 2 the progress of the reaction front with time in the bed is depicted. In this figure the wavelike behavior of the bulk concentration profile reveals the small effect of dispersive process. The CPU time for obtaining the gas profile in $\tau_{vol} = 600$ was 4.86×10^{3} sec using a Pentium 4 CPU 3.00 GHz.

The solid conversion in each solid spherical pellet is calculated by the following equation:

$$X(\tau) = 1 - 3\int_{0}^{1} \rho^{2} b \, d\rho \tag{18}$$

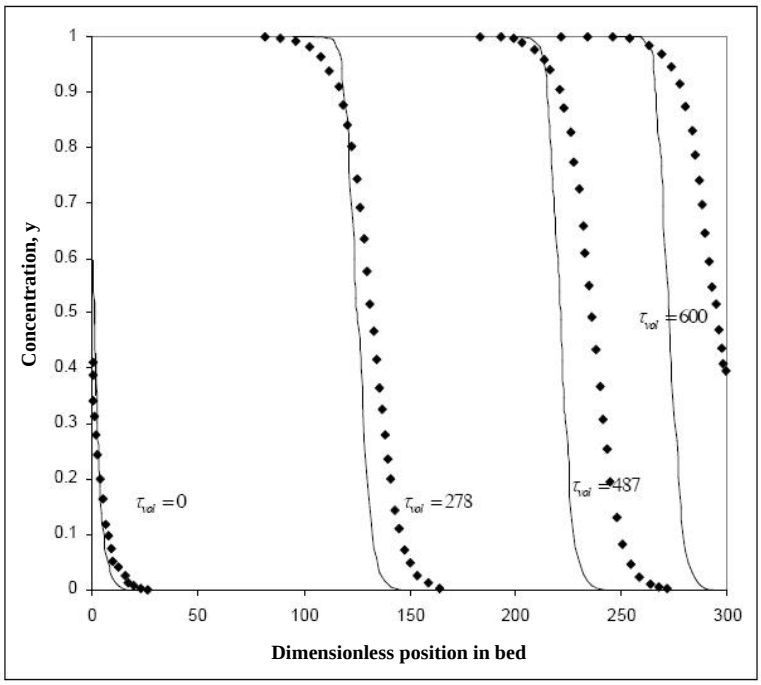

Figure 2. comparison of this work (continuous lines) with the results of Ref. [26] (dotted points) for dimensionless bulk gas concentration. $\phi_{vol} = 10, Bi = 50, Pe = 1.1, \beta = 3.3$

Fig. 3 is the solid reactant concentration versus the length of the bed at various times. The movement of the reaction front is being observed in this figure too. Fig. 4 shows the strong effect of reaction Thiele modulus on the breakthrough curve. It also shows that when the reaction Thiele modulus is high, the unreacted gaseous appear sharply in the outlet of the reactor. In other words, in the case of high reaction Thiele modulus, the reacted solid zone becomes larger in the reactor with a plug manner. There is acceptable agreement between the behaviour of the results of this work and the results of Ref. [26] in these Figures.

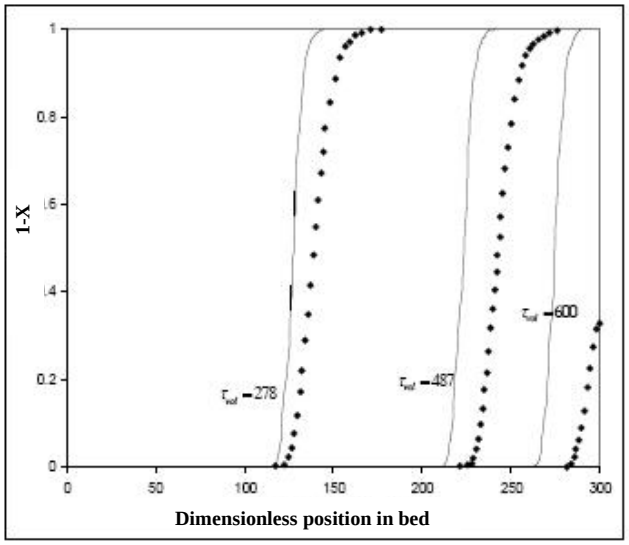

Figure 3. comparison of this work (continuous lines) with the results of Ref. [26] (dotted points) for unreacted solid conversion. $\phi_{vol} = 10, Bi = 50, \quad Pe = 1.1, \beta = 3.3$

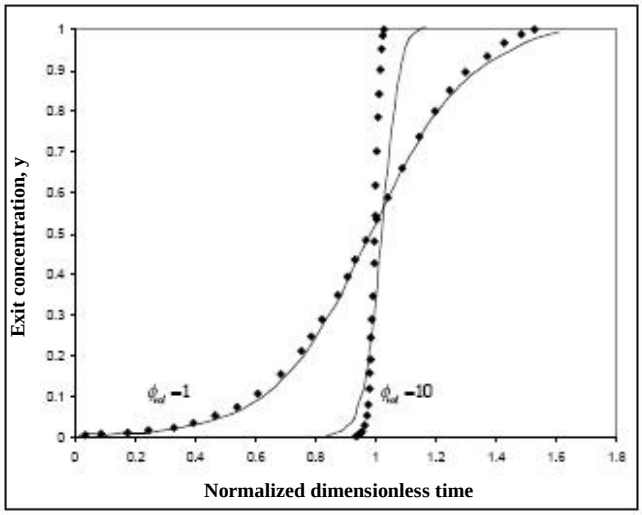

Figure 4. comparison of this work (continuous lines) with the results of Ref. [26] (dotted points). Effect of the reaction Thiele modulus on the shape of breakthrough curve. $Bi = 50, Pe = 1.1, \quad \beta = 3.3, L = 300$

4.2. Random pore model

The random pore model which has been established by Bhatia and Perlmutter [30,31] is considered in this part. This model includes transport effects arising from boundary layer, intraparticle and product layer diffusion. In addition, the structural behavior of the solid is predicted by this model. In most of the gas-soild reactions, the structural behavior of the solid is a function of the reaction products. When solid products are formed during the reaction, the structural changes depend on the ratio of the molar volumes of the solid product and solid reactant. Depending on the value of this parameter (Z), two major cases are found. When Z is less than unity, the reactions are characterized by a gradual increase in porosity and pore sizes. For instance, the gasification reactions show this condition. When Z is larger than unity, the reactions are characterized by a gradual increase in solid volume leading to decrease in porosity and even pore plugging for high Z values. An example of this case is the elimination of sulfur dioxide from coal based power plants with lime or limestone [32,7]. In the presence of significant intraparticle diffusional limitations, the overall picture of the reaction of calcined limestone with SO_2 becomes more complex. Since there is a higher rate of reaction at the external surface of the particles, complete pore closure may first take place at the external surface of the solid while there are still open pore spaces remaining in the interior. The random pore model predicts these behaviors very well. The application of this model for the reaction of a single particle of lime with SO_2 showed acceptable results [33].

The sulphation of calcined limestone particles in a packed bed will be taken here as a case study to predict the behaviour of pore plugging along the bed. The stoichiometry of this reaction is given by:

$$CaO(s)+SO_2(g)+\tfrac{1}{2}O_2(g)\rightarrow CaSO_4(s) \tag{19}$$

The solid volume increase by a factor of 3.09 during this reaction [34]. Experimental investigations indicate that in excess of oxygen, this reaction is first order with respect to the partial pressure of sulphur dioxide [34,35]. Moreover, on the grounds that the concentration of sulphur dioxide in flue gases is generally less than 0.5% in volume [34,36,37], the small volume changes in the gas phase suggests that negligible pressure gradients develop within the particle [32].

In this model, Eq. (5) becomes:

$$\frac{1}{\rho^2}\frac{\partial}{\partial\rho}\left(\delta\rho^2\frac{\partial\zeta}{\partial\rho}\right)=\frac{\phi_R^2\,\zeta\, b\sqrt{1-\psi\ln b}}{1+\dfrac{\Omega Z}{\psi}\left[\sqrt{1-\psi\ln b}-1\right]} \tag{20}$$

Consequently Eq. (8) takes the following form:

$$\frac{\partial b}{\partial\tau}=-\frac{\zeta\, b\sqrt{1-\psi\ln b}}{1+\dfrac{\Omega Z}{\psi}\left[\sqrt{1-\psi\ln b}-1\right]} \tag{21}$$

The solid conversion in this model can be calculated for spherical pellet as follows:

$$X(\tau)=1-3\int_0^1\rho^2 b.d\rho \tag{22}$$

The parameter δ in Eq. (20) plays the role of relating the diffusion coefficient to the pellet porosity. There are two approaches for relating the diffusion to the pellet porosity . The first approach is from Wakao and Smith [38]:

$$\delta = \frac{D_e}{D_{e0}} = \left(\frac{\varepsilon}{\varepsilon_0}\right)^2 = \left[1 - \frac{(Z-1)(1-\varepsilon_0)(1-b)}{\varepsilon_0}\right]^2 \quad (23)$$

The second approach assumes that tortuosity factor of the pellet remains constant during the reaction. The result of this approach is as follows:

$$\delta = \frac{D_e}{D_{e0}} = \left(\frac{\varepsilon}{\varepsilon_0}\right) = \left[1 - \frac{(Z-1)(1-\varepsilon_0)(1-b)}{\varepsilon_0}\right] \quad (24)$$

Once the value of δ at the external surface of the solids along the bed becomes very small, the diffusion of the gaseous reactant into the inner parts of the pellets will be stopped. Consequently these solid particles play the role of inert particles in the bed after surface blockage. Figs. 5, 6 and 7 are the results of this work for the sulfation of the calcined limestone in a packed bed. The dimensionless parameters of the pellets in this section are obtained from the experimental works of Hartman and Coughlin [34]. Moreover, Eq. (24) has been employed in these figures. Fig. 5 is the bulk concentration at different times along the bed. This figure shows the progress of the bulk concentration along the bed. The complete execution time for $\tau_R = 370$ in Fig. 5 was 5.32×10^3 sec using a pentium 4 CPU 3.00 GHz. Fig. 6 is the solid conversion of the bed at different times. This figure shows the expected incomplete solid conversion. Fig. 6 shows that by the progress of the reaction, only 40% of each solid particle is being converted while the inner parts of the pellets (60%) remain unaffected due to the surface pore closure along the bed. This result is in close agreement with the experimental result of Ref. [34] for the reaction of single particle pellet. Fig. 7 is the breakthrough curve using experimental data of Ref. [34]. This figure shows the behaviour of unreacted outlet gaseous versus dimensionless time. Figs. 8, 9 and 10 have the same results for higher (approximately two times larger than the previous one) reaction Thiele modulus with the aid of Eq. (24). Again, the dimensionless parameters of solid particles are obtained from one of the experimental works of Ref. [34]. Fig. 8, which shows the bulk concentration, becomes sharper with respect to Fig. 5. Fig. 9 reveals the incomplete solid conversion along the bed i.e., about 77% of each solid particle remains unreacted due to the pore plugging. This unreacted portion of pellets is greater than unreacted portion of the pellets reported in Fig. 6. Results of solid conversion along the column in Fig. 9 satisfies the experimental work of Hartman and Coughlin [34] for the reaction of the same single solid particle successfully. Considering Figs. 7 and 10, the effect of reaction Thiele modulus on the breakthrough curve is observed. The more the reaction Thiele modulus, the sharper the breakthrough curve.

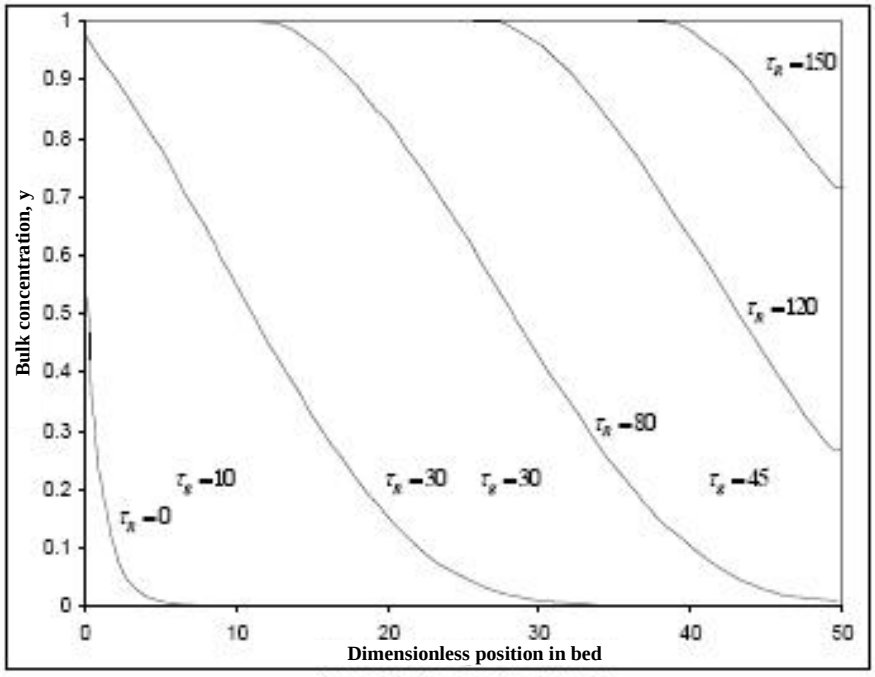

Figure 5. development of the bulk gas concentration profiles in the case of random pore model.
$\phi_R = 21.3, Pe = 1.1,\ Bi = 50, \beta = 3.3, Z = 3.09,\ \Omega = 185, \psi = 2.5, \varepsilon_0 = 0.52$

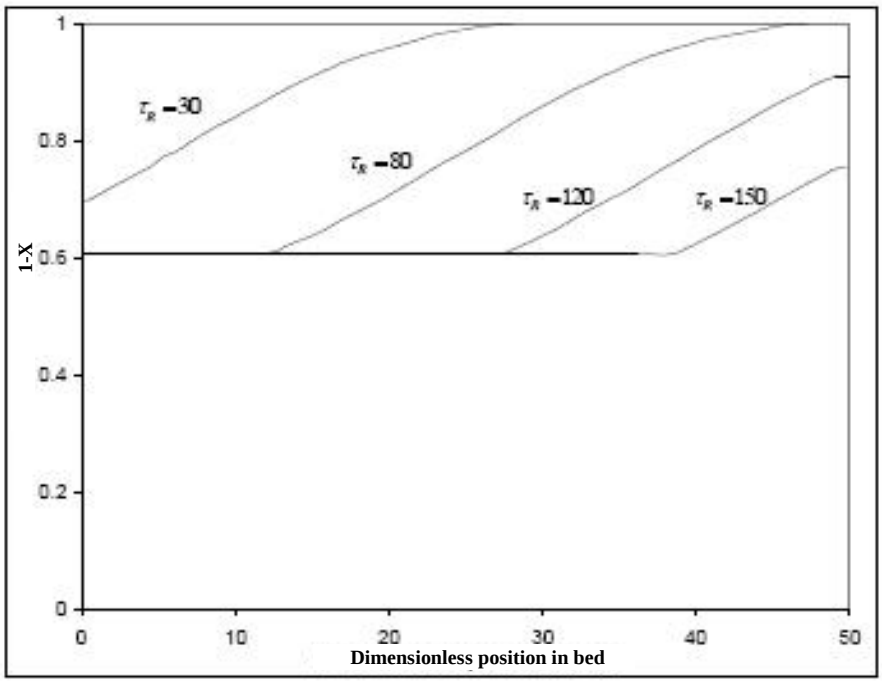

Figure 6. concentration profiles of the solid reactant in the case of random pore model.
$\phi_R = 21.3,\ Pe = 1.1,\ Bi = 50,\ \beta = 3.3,\ \ Z = 3.09,\ \ \Omega = 185,\ \ \psi = 2.5, \varepsilon_0 = 0.52$

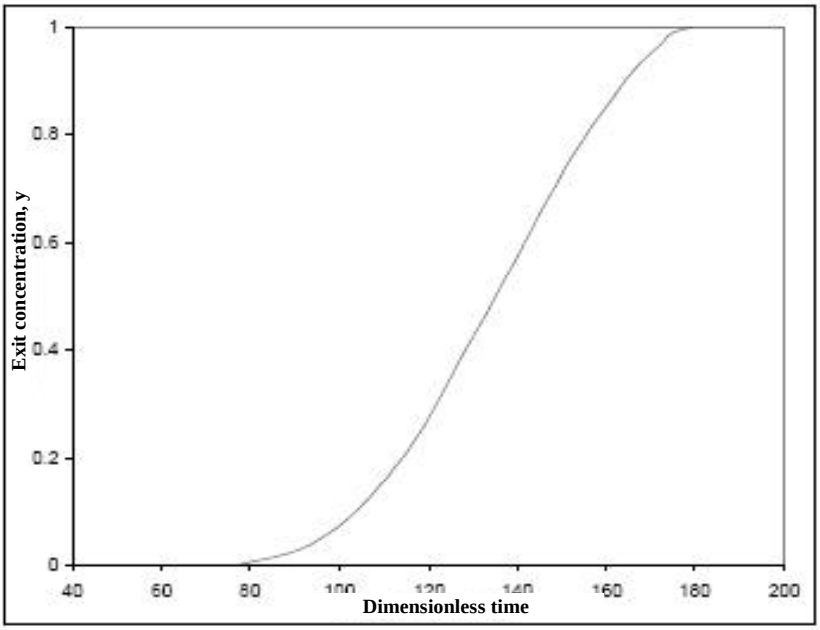

Figure 7. breakthrough curve for the random pore model. $\phi_R = 21.3, Pe = 1.1, Bi = 50, \beta = 3.3, Z = 3.09,$ $\Omega = 185, \psi = 2.5, \varepsilon_0 = 0.52, L = 50$

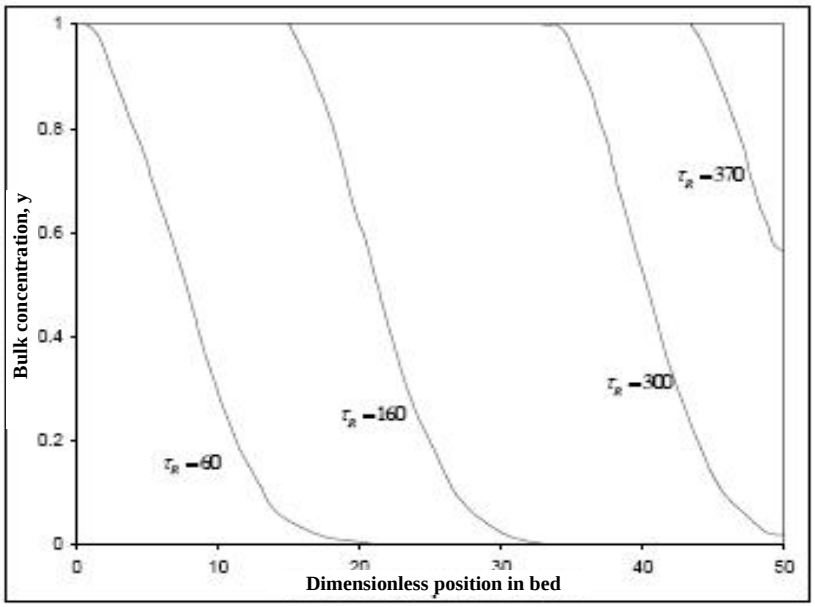

Figure 8. development of the bulk gas concentration profiles in the case of random pore model. $\phi_R = 50, Pe = 1.1, Bi = 50, \beta = 3.3, Z = 3.09, \Omega = 185, \quad \psi = 2.5, \varepsilon_0 = 0.52$

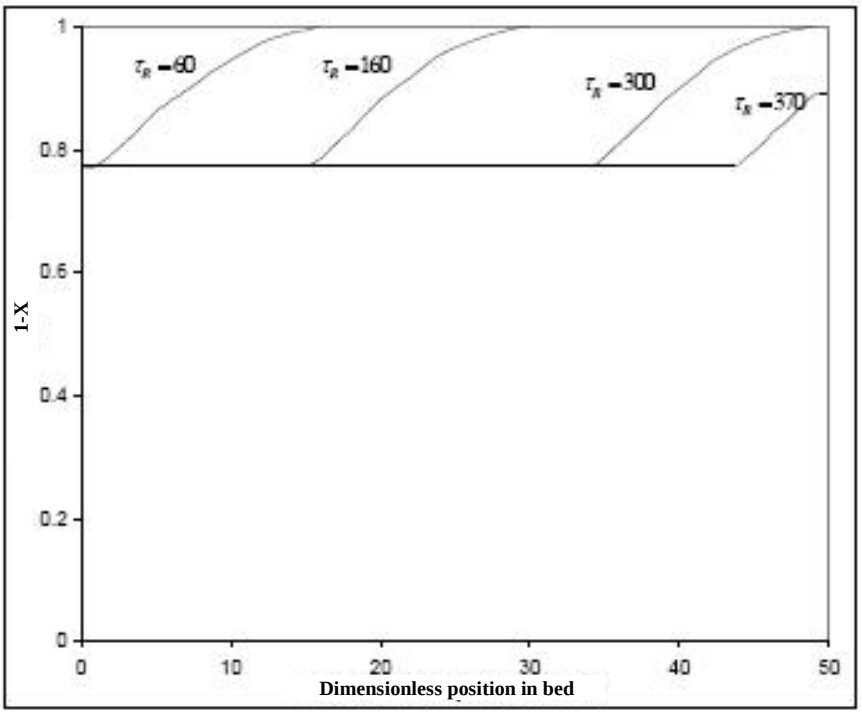

Figure 9. concentration profiles of the solid reactant in the case of random pore model.
$\phi_R = 50, Pe = 1.1, Bi = 50, \beta = 3.3, Z = 3.09, \Omega = 185, \quad \psi = 2.5, \varepsilon_0 = 0.52$

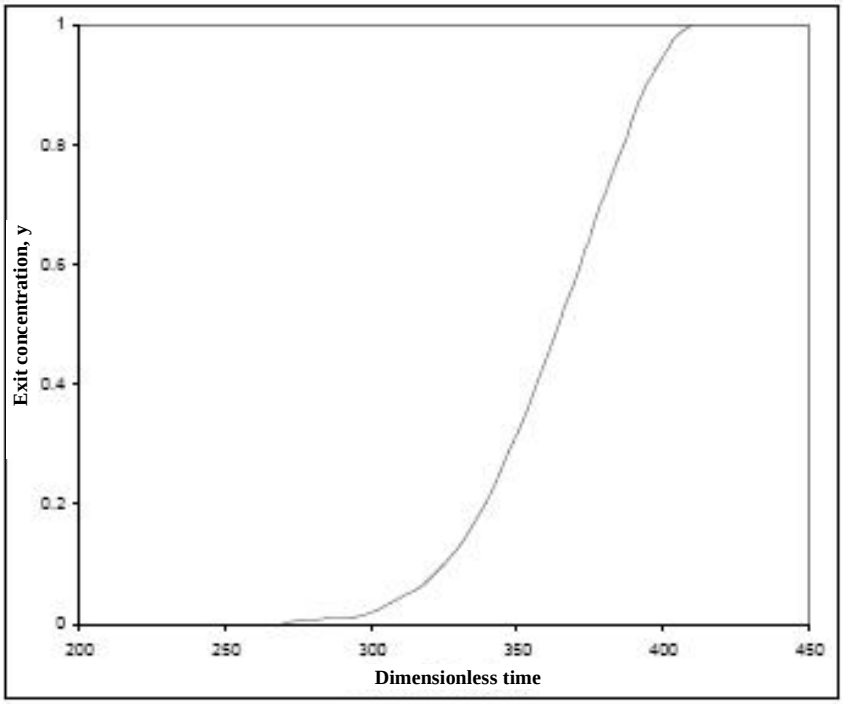

Figure 10. breakthrough curve for the random pore model. $\phi_R = 50, Pe = 1.1, Bi = 50, \beta = 3.3, Z = 3.09,$
$\Omega = 185, \psi = 2.5, \varepsilon_0 = 0.52, L = 50$

Figs. 11, 12 and 13 are the predictions of random pore model in a packed column for $Z = 1.6$. This level of Z is suitable for the reaction of H_2S+ZnO. The sulfation of zinc oxide is a noncatalytic gas-solid reaction characterized by the formation of a solid product (ZnS). This solid product occupies more space than the solid reactant [8]. Zinc oxide is known to react with hydrogen sulfide over a wide range of temperature and pressure. The removal of trace H_2S from sweet natural gas which is the feed of synthesis plants is important for preventing the nickel catalyst poisoning [9]. In addition, the H_2S of the product gases in the coal gasification plants is being removed by packed bed of zinc oxide. In this part, a typical reaction with the expansion factor of 1.6 is considered in a packed bed reactor.

Fig. 11 is the bulk concentration along the bed. Considering this figure, although there is not complete pore plugging at the surface of the pellets, the diffusion of the reactant gas to the interior of the pellets becomes harder by the progress of the reaction but it will never completely stop. In other words, due to the decreasing of the diffusion coefficient (see Eq. (23)), considerable time is required for complete conversion of the solid pellets in each row of the packed column. The effect of this phenomenon can be briefly observed in Fig.(12). As an illustration, in this figure, at $\tau = 650$ the solid conversion of the pellets at the first row of the bed ($\xi = 0$) reaches 89% (11% unreacted). Fig. 13 is the breakthrough curve for the random pore model with $Z = 1.6$ (for instance for the case of H_2S+ZnO).

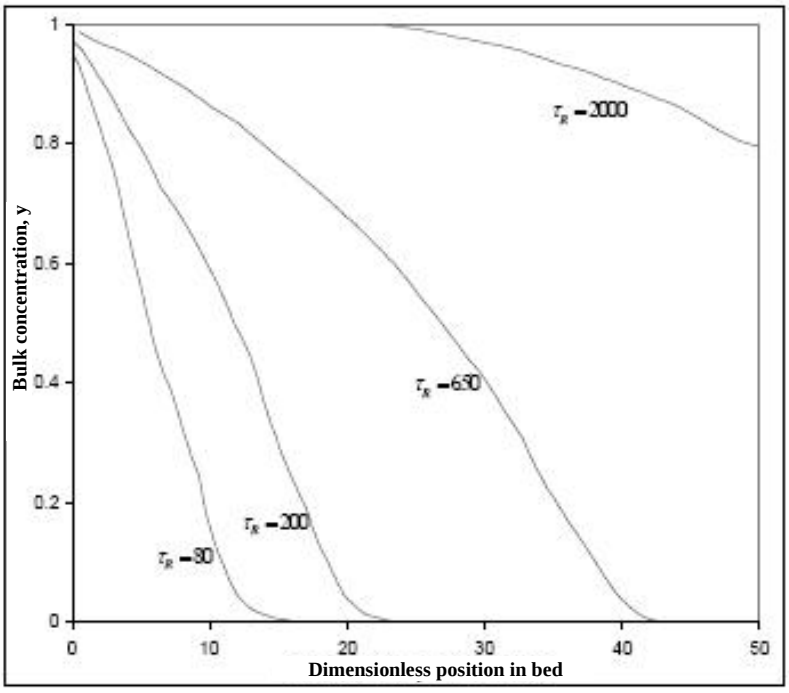

Figure 11. development of the bulk gas concentration profiles in the case of random pore model.

$\phi_R = 50, Pe = 1.1, Bi = 50, \beta = 3.3, Z = 1.6, \Omega = 1, \psi = 1, \quad \varepsilon_0 = 0.5$

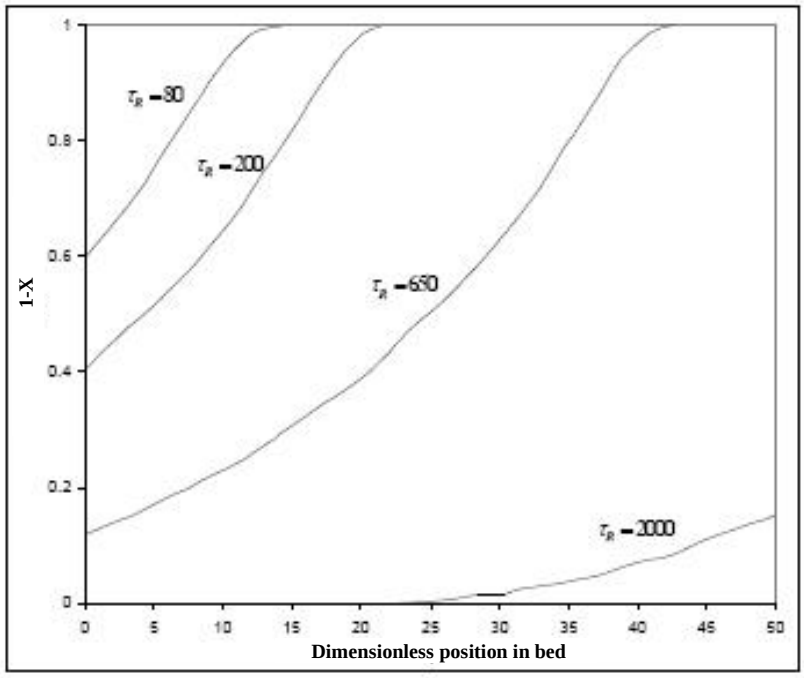

Figure 12. concentration profiles of the solid reactant in the case of random pore model.
$\phi_R = 50, Pe = 1.1, Bi = 50, \beta = 3.3, Z = 1.6, \Omega = 1, \psi = 1, \quad \varepsilon_0 = 0.5$

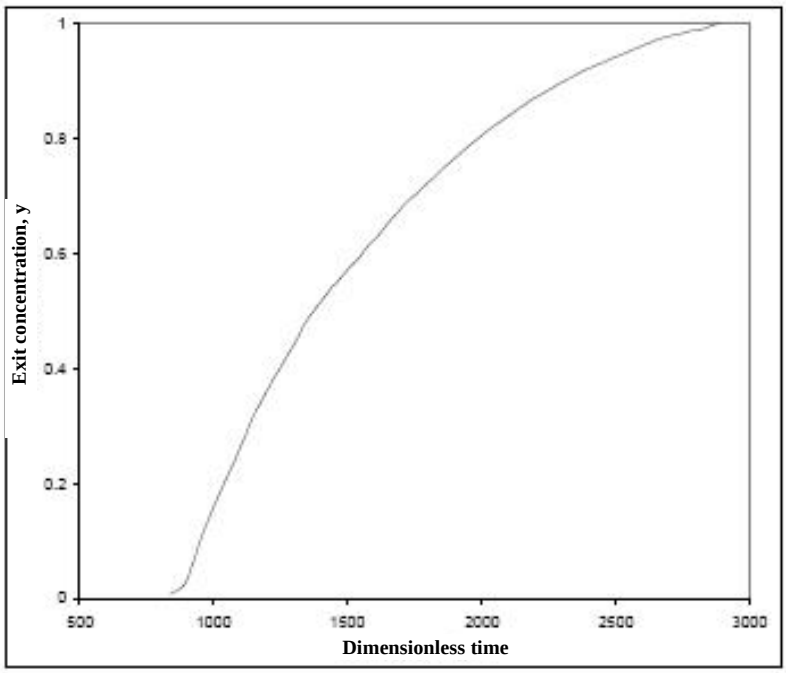

Figure 13. breakthrough curve for the random pore model. $\phi_R = 50, Pe = 1.1, Bi = 50,$
$\beta = 3.3, Z = 1.6, \Omega = 1, \psi = 1, \varepsilon_0 = 0.5, L = 50$

5. Conclusions

The governing partial differential equations of the packed bed reactor have been solved by Rayleigh-Ritz finite element method successfully. The finite element method is the most powerful computer oriented method ever devised to analyze practical engineering problems such as reactors. Thus the finite element method can be very useful for solving the governing equations of the packed bed reactors for predicting the behaviour of the reactants and products which help us to design (and/or scaling up) more efficient packed bed reactors.

Nomenclature

$b = \frac{c_B}{c_{B0}}$	dimensionless solid reactant concentration
$Bi = \frac{k_m R_p}{D_e}$	pellet Biot number
c	gas concentration in the bulk phase
c_0	initial gas concentration in the bulk phase
c_B	solid reactant concentration
c_{B0}	initial solid reactant concentration
c'	gas concentration within the solid pellet
D_e	effective diffusivity within the pellet
D_{e0}	initial effective diffusivity within the pellet
D_L	axial dispersion coefficient within the bed
D_P	effective diffusivity of the gas in the product layer
e	bed void fraction
k_m	mass transfer coefficient
k	reaction rate constant
L	total length of the bed
M_B	molecular weight of the solid reactant
M_D	molecular weight of the solid product
$Pe = \frac{u R_p}{D_L}$	pellet Peclet number
r	radial distance in pellet
R_p	pellet radius
S_0	reaction surface area per unite volume
t	time
u	interfacial velocity
x	axial distance from front of the bed
X	solid conversion of the pellets
$y = \frac{c}{c_0}$	dimensionless bulk gas concentration
$Z = \frac{\upsilon_D \rho_B M_D}{\upsilon_B \rho_D M_B}$	ratio of molar volumes of the solid product to the solid reactant

Greek letters

ε	pellet porosity
ε_0	initial pellet porosity
$\xi = \frac{x}{R_p}$	dimensionless distance from front of the bed
$\zeta = \frac{c'}{c_0}$	dimensionless gas concentration within the pellet
$\Lambda = \frac{L}{R_p}$	dimensionless total length of the bed

$\rho = \frac{r}{R_p}$ dimensionless radial distance within pellet

ρ_B density of solid reactant

ρ_D density of solid product

$\tau_{vol} = \upsilon_B \frac{k\, c_0\, t}{1-X}$ dimensionless time for the volume reaction model

$\tau_R = \frac{k\, c_0\, S_0}{(1-\varepsilon_0)} t$ dimensionless time for the random pore model

$\phi_{vol} = R_p \sqrt{\frac{\upsilon_A\, k}{D_e}}$ reaction Thiele modulus for volume reaction model

$\phi_R = R_p \sqrt{\frac{k\, \rho_B\, S_0}{M_B\, \upsilon_B D_{e0}}}$ reaction Thiele modulus for random pore model

ψ structural parameter in random pore model

$\Omega = \frac{2k\, \rho_B (1-\varepsilon_0)}{M_B\, \upsilon_B\, D_P\, S_0}$ product layer resistance in random pore model

$\beta = \frac{(1-e)}{e} \frac{3k_m\, R_p}{D_L}$ dimensionless parameter in Eq. (2)

References

[1] Evans, J. W., Song, S. and Leon Surce, C. E., "The kinetic of nickel oxide reduction by hydrogen measurements in a fluidized bed and in a gravimetric apparatus". Metall. Trans., B7 (1), 55 (1976).

[2] Ale Ebrahim, H. and Jamshidi, E., "Kinetic study and mathematical modeling of the reduction of ZnO-PbO mixtures by methane", Ind. Eng. Chem. Res., 44 (3), 495 (2005).

[3] Alizadeh, R., Jamshidi, E. and Ale Ebrahim, H., "Kinetic study of nickel oxide reduction by methane", Chem. Eng. Tech., 30 (8), 1123 (2007).

[4] Kimura, S., "Oxidation kinetics of polycrystalline zinc sulfide grains", AIChE J., 35 (2), 339 (1989).

[5] Parasad, S. and Pandey, B. D., "Sulphation roasting studies on synthetic copper-iron sulfides with steam and oxygen", Canadian Metallurgical Quarterly., 38 (4), 237 (1999).

[6] Kocaefe, D., Karman, D. and Steward, F. R., "Interpretation of the sulfation rate of CaO, MgO and ZnO with SO_2 and SO_3", AIChE J., 33 (11), 1835 (1987).

[7] Zarkanitis, S., Sotirchos, S. V., "Pore structure and particle size effects on limestone capacity for SO_2 removal", AIChE J., 35 (5), 821 (1989).

[8] Efthimiadis, E. A. and Sotirchos, S. V., "Reactivity evolution during sulfation of porous zinc oxide", Chem. Eng. Sci., 48 (5), 829 (1993).

[9] Gibson, J. B. and Harrison, D. P., "The reaction between hydrogen sulfide and spherical pellets of zinc oxide", Ind. Eng. Chem. Process Des. Dev., 19 (2), 231 (1980).

[10] Ale Ebrahim, H. and Jamshidi, E., "Synthesis gas production by zinc oxide reaction with methane: elimination of greenhouse gas emission from a metallurgical plant", Energy Conv. Manag, 45 (3), 345 (2004).

[11] Jamshidi, E. and Ale Ebrahim, H., "A

new clean process for barium carbonate preparation by barite reduction with methane", Chem. Eng. Processing, 47 (9-10), 1567 (2008).

[12] Lu, G. Q. and Do, D. D., "A kinetic study of coal reject-derived char activation with CO_2, H_2O and air", Carbon., 30 (1), 21 (1992).

[13] Castello, D. L., Amoros, D. C. and Solano, A. L., "Powdered activated carbons and activated carbon fibers for methane storage: A comparative study", Energy and Fuels., 16 (5), 1321 (2002).

[14] Hashimoto, K. and Silvestone, P. L., "Gasification: part I. Isothermal kinetic control model for a solid with a pore size distribution", AIChE J., 19 (2), 259 (1973).

[15] Delikournas, E. A. and Perlmutter, D. D., "Combined effects of mass transfer and inaccessible porosity in gasification reactions", AIChE J., 39 (5), 829 (1993).

[16] Ruthven, D. M., Principles of adsorption and adsorption processes, Wiley, New York, USA, (1984).

[17] Yang, R. T., Gas separation by adsorption processes, Butterworths, Boston, USA, (1986).

[18] Szekely, J., Evans, J. W. and Sohn, H. Y., Gas–Solid Reactions, Academic Press, New York, USA, (1976).

[19] Del Borghi, M., Dunn, J. C. and Bischoff, K. B., "A technique for solution of the equations for fluid solid reactions with diffusion", Chem. Eng. Sci., 31 (11), 1065 (1976).

[20] Dudukovic, M. P. and Lamba, H. S., "Solution of moving boundary problems for gas-solid noncatalytic reactions by orthogonal collocation", Chem. Eng. Sci., 33 (3), 303 (1978).

[21] Afshar Ebrahimi, A., Ale Ebrahim, H. and Jamshidi, E., "Solving partial differential equations of gas–solid reactions by orthogonal collocation", Comp. & Chem. Eng., 32 (8), 1746 (2008).

[22] Calvelo, A. and Smith, J. M., "Intrapellet transport in gas–solid non-catalytic reactions", Proceedings of the Chemca 70, Butterworth, Australia, Paper 3.1 (1971).

[23] Ramachandran, P. A. and Doraiswamy, L. K., "Modeling of noncatalytic gas-solid reactions", AIChE J., 28 (6), 881 (1982).

[24] Evans, J. W. and Rande, M. G., "The grain model for reaction between a gas and a porous solid- a refined approximate solution to the equations", Chem. Eng. Sci., 35 (5), 1261 (1980).

[25] Liapis, A. I. and Rippin, D. W. T., "The simulation of binary adsorption in activated carbon columns using estimates of diffusional resistance within the carbon particles derived from batch experiments", Chem. Eng. Sci., 33 (5), 593 (1978).

[26] Fernandes, N. and Gavalas, G. R., "Solution of equations describing fluid-solid reactions in packed columns", AIChE J., 41 (12), 2549 (1995).

[27] Bhatia, S. K., "On the pseudo steady state hypothesis for fluid solid reactions"., Chem. Eng. Sci., 40, 868 (1985).

[28] Reddy, J. N., An Introduction to the Finite Element Method, McGraw-Hill, New York, USA, (2006).

[29] Reddy, J. N., An Introduction to Nonlinear Finite Element Analysis, Oxford University Press, New York, USA, (2004).

[30] Bhatia, S. K. and Perlmutter, D. D., "A random pore model for fluid–solid reactions: I. Isothermal, kinetic control", AIChE J., 26 (3), 379 (1980).

[31] Bhatia, S. K. and Perlmutter, D. D., "A random pore model for fluid–solid reactions: II. Diffusion and transport effects", AIChE J., 27 (2), 247 (1981).

[32] Reyes, S. and Jensen, K. F., "Percolation concepts in modeling of gas-solid reactions-III. Application to sulphation of calcined limestone", Chem. Eng. Sci., 42 (3), 565 (1987).

[33] Bhatia, S. K. and Perlmutter, D. D., "The effect of pore structure on fluid-solid reactions: applications to the SO_2-Lime reaction", AIChE J., 27 (2), 226 (1981).

[34] Hartman, M. and Coughlin, R. W., "Reaction of sulfur dioxide with limestone and the grain model", AIChE J., 22 (3), 490 (1976).

[35] Dogu, T., "The importance of pore structure and diffusion in the kinetics of gas-solid noncatalytic reactions: Reaction of calcined limestone with SO_2", Chem. Eng. J., 21 (3), 213 (1981).

[36] Potter, A. E., "Sulfur oxide capacity of limestone", Ceramic Bull., 48, 855 (1969).

[37] Borgwardt, R. H., "Kinetics of the reaction of SO_2 with calcined limestone", Env. Sci. Tech., 4 (1), 59 (1970).

[38] Wakao, N. and Smith, J. M., "Diffusion in catalyst pellets", Chem. Eng. Sci., 17 (11), 825 (1962).